

Phase field model of premelting of grain boundaries

Alexander E. Lobkovsky

Physics Department, Northeastern University, Boston, MA

James A. Warren

National Institute of Standards and Technology, Gaithersburg, MD

We present a phase field model of solidification which includes the effects of the crystalline orientation in the solid phase. This model describes grain boundaries as well as solid-liquid boundaries within a unified framework. With an appropriate choice of coupling of the phase field variable to the gradient of the crystalline orientation variable in the free energy, we find that high angle boundaries undergo a premelting transition. As the melting temperature is approached from below, low angle grain boundaries remain narrow. The width of the liquid layer at high angle grain boundaries diverges logarithmically. In addition, for some choices of model coupling, there may be a discontinuous jump in the width of the fluid layer as function of temperature.

I. INTRODUCTION

Understanding the structure of a boundary between two crystalline grains is a prerequisite to building theories of microstructure development and evolution. Even in pure materials, there are many possibilities for this structure. Whereas a low angle grain boundary may be thought of as an array of dislocations [1], this description is not always accurate or useful. Several molecular dynamics studies indicated that grain boundaries develop a layer of disordered, amorphous material as the temperature is raised [2, 3, 4, 5]. Within a few degrees of the melting temperature T_m , grain boundaries in pure aluminum liquefy [6]. The directly measured width of the liquid layer was consistent with a divergence at T_m . Careful calorimetry measurements as in [7] may be able to pin down the nature of the divergence. Measurements of the dihedral angle of the bicrystal in contact with the melt in bismuth [8, 9, 10] uncovered a discontinuous transition as a function of misorientation of tilt boundaries near the melting point.

Indirect probes of the structure of grain boundaries also find evidence of a structural transition. Measurements of grain boundary mobility [11], shear resistance [12] and diffusion coefficients [13] all found discontinuous jumps in these quantities at some characteristic temperature below the melting point.

Melting at a grain boundary as well as surface melting [14] is a particular case of a broad class of wetting phenomena [15]. Generally, interfacial melting may be complete (the width of the liquid layer diverges as $T \rightarrow T_m$) or incomplete (it stays finite) depending on the functional dependence of the free energy on the thickness of the liquid layer. There may also be a discontinuous jump in the width of the liquid layer as a function of temperature.

An explicit calculation of the free energy of a liquid layer is difficult and has been performed only in a few cases. For example, Kikuchi and Cahn calculated the free energy of a disordered grain boundary within a lattice gas model [16]. They concluded that when the interaction of the solid-liquid interfaces is short range, the transition,

if it exists, is continuous and the width of the liquid film diverges as a logarithm of the undercooling. Elbaum and Schick calculated the energy of a water film on ice due to the van der Waals dispersion forces [17] and concluded that premelting there is incomplete.

In this paper we study the modification of the phase field model of grain boundaries [18]. Our model treats solidification as well as grain boundaries within a unified consistent framework. Therefore, we ought to be able to describe melting of grain boundaries. The present authors elucidated the general properties of this model in Ref. [19]. There we were able to compute, in the limit of an infinitely sharp interface, the energy, width and mobility of model grain boundaries.

We hope to use the predictions of our phase field model near the melting point to pin down the correct/realistic form of the model coupling functions which offer the essential flexibility in our model. We apply the results of [19] and indeed find that grain boundaries undergo complete or incomplete continuous premelting transition depending on the misorientation of the two grains. In addition, for a particular choice of the model coupling functions, there is a discontinuous jump in the boundary width as a function of temperature.

In the following Section II we briefly describe the phase field model of grain boundaries (for a better discussion see Ref. [19]). In Sec. III we apply the results of [19] to the modified model. We consider the structure composed of the grain boundary plus the layer of liquid and calculate its energy and width. We find that high angle grain boundaries undergo a continuous premelting transition. We also find that for a particular choice of the model coupling functions, there is a discontinuous jump in the width of the liquid layer for some boundaries. In the next Sec. IV, we show that the existence of a liquid layer greatly affects the grain boundary migration. We summarize our findings in Sec. V.

II. MODEL

The phase field ϕ is introduced in standard treatments of the kinetics of the liquid-solid transition [20]. It measures the degree of structural disorder. Conventionally $\phi = 1$ corresponds to a perfect solid while $\phi = 0$ corresponds to a liquid. In [18] Kobayashi Warren and Carter introduced η which measures the degree of orientational disorder. We postulate that these two order parameters are essentially the same. Therefore the bulk free energy density [19] $f(\phi)$ in the free energy \mathcal{F}

$$\mathcal{F}[\phi, \theta] = \frac{1}{\epsilon} \int_{\Omega} dA \left[f(\phi) + \frac{\alpha^2}{2} |\nabla\phi|^2 + g(\phi) s |\nabla\theta| + h(\phi) \frac{\epsilon^2}{2} |\nabla\theta|^2 \right], \quad (1)$$

should be thought of as a double well with minima at $\phi = 0, 1$. Here θ is the local crystal orientation and α , ϵ and s are positive model parameters. The model coupling functions $g(\phi)$ and $h(\phi)$ must vanish in the fluid $\phi = 0$ since the orientation θ has no meaning there and therefore its gradients should not be penalized.

The present authors analyzed the gradient flow of this free energy

$$Q(\phi, \nabla\theta) \tau_{\phi} \frac{\partial\phi}{\partial t} = \alpha^2 \nabla^2 \phi - f_{\phi} - g_{\phi} s |\nabla\theta| - h_{\phi} \frac{\epsilon^2}{2} |\nabla\theta|^2, \quad (2a)$$

$$P(\phi, \nabla\theta) \tau_{\theta} \phi^2 \frac{\partial\theta}{\partial t} = \nabla \cdot \left[h \epsilon^2 \nabla\theta + g s \frac{\nabla\theta}{|\nabla\theta|} \right], \quad (2b)$$

in Ref. [19]. We used the subscripts to denote differentiation except for the time constants τ_{η} and τ_{θ} . The mobility functions P and Q must be positive definite, but are otherwise unrestricted.

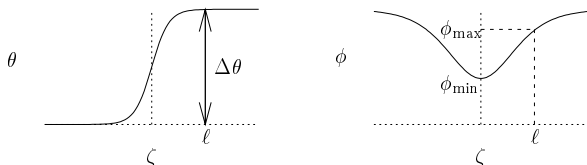


FIG. 1: Order parameters in a flat stationary grain boundary as a function of the coordinate ζ normal to the boundary. The orientation θ varies smoothly between 0 and $\Delta\theta$ in the grain boundary $\zeta \in [-\ell, \ell]$ and is constant in the interior of the grains. The phase field ϕ approaches 1 exponentially away from the boundary.

In Ref. [19] we computed the structure of the boundary, its energy and mobility the limit of a sharp interface. Let us briefly summarize these results here. The structure of the boundary is shown in Fig. 1. The values of the phase field ϕ in the center of the grain boundary ϕ_{\min} and at the edge of the grain boundary ϕ_{\max} are found by solving

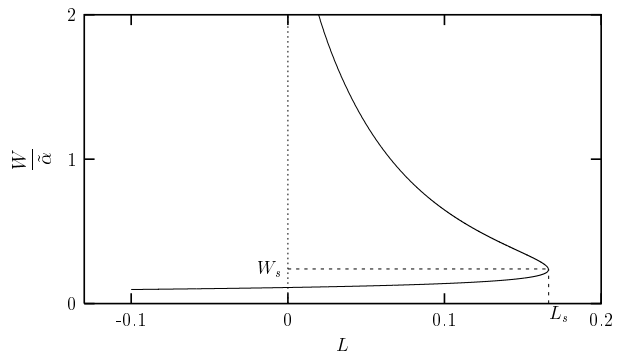


FIG. 2: Amount of liquid W in units of $\tilde{\alpha}$ a function of temperature L for a low-angle grain boundary. $h = \phi^2$, $\tilde{s} = 1$ and $\Delta\theta/\tilde{\alpha} = 0.1$.

the following two equations [19]

$$g(\phi_{\max}) = g(\phi_{\min}) + \frac{\sqrt{2f(\phi_{\min})h(\phi_{\min})}}{\tilde{s}}, \quad (3)$$

$$\frac{\Delta\theta}{2\tilde{\alpha}\tilde{s}} = \int_{\phi_{\min}}^{\phi_{\max}} \frac{d\phi (g(\phi_{\max}) - g)}{h\sqrt{2f - \tilde{s}^2(g(\phi_{\max}) - g)^2/h}}, \quad (4)$$

where $\tilde{\alpha} = \alpha/\epsilon$ and $\tilde{s} = s/\epsilon$. Once ϕ_{\min} and ϕ_{\max} are determined, we can compute the energy of the grain boundary γ_{gb} and the amount of “fluid” or disordered material at the interface W via

$$\gamma_{\text{gb}} = \tilde{s}\Delta\theta g(\phi_{\max}) + 2\tilde{\alpha} \int_{\phi_{\max}}^1 d\phi \sqrt{2f} + 2\tilde{\alpha} \int_{\phi_{\min}}^{\phi_{\max}} d\phi \sqrt{2f - \tilde{s}^2(g(\phi_{\max}) - g)^2/h}, \quad (5)$$

$$W \equiv \int_0^{\infty} d\zeta (1 - \phi) = \tilde{\alpha} \int_{\phi_{\max}}^1 \frac{d\phi (1 - \phi)}{\sqrt{2f}} + \tilde{\alpha} \int_{\phi_{\min}}^{\phi_{\max}} d\phi \frac{1 - \phi}{\sqrt{2f - \tilde{s}^2(g(\phi_{\max}) - g)^2/h}}. \quad (6)$$

III. FLAT STATIONARY BOUNDARY

Equipped with the way of calculating measurable properties of the grain boundary in our model we make choices for the coupling functions and explore the results of the calculation. As we alluded to before the bulk free energy density $f(\phi)$ is a double well which we choose to be [20]

$$f(\phi) = \frac{\phi^2(1 - \phi)^2}{2} - L(1 - \phi)^3(1 + 3\phi + 6\phi^2), \quad (7)$$

where $L = -f(0)$ is linear in the temperature deviation from the melting point $T - T_m$. The choices of $g(\phi)$ and $h(\phi)$ are more flexible. These functions provide the essential freedom in our model. The only constraint on them is that they must vanish sufficiently quickly at

$\phi = 0$. For example, they can be chosen [18] to match the Read-Shockley [21] misorientation dependence of the grain boundary energy. In this paper we will set

$$g(\phi) = \phi^2, \quad (8)$$

and explore two choices for h

$$h_1(\phi) = \phi^2 \quad \text{and} \quad h_2(\phi) = 1. \quad (9)$$

The second choice is problematic since it ascribes an energy cost to changes of orientation in the liquid where it has no meaning. We nevertheless explore its implications to gain insight and intuition into the role of the model function h .

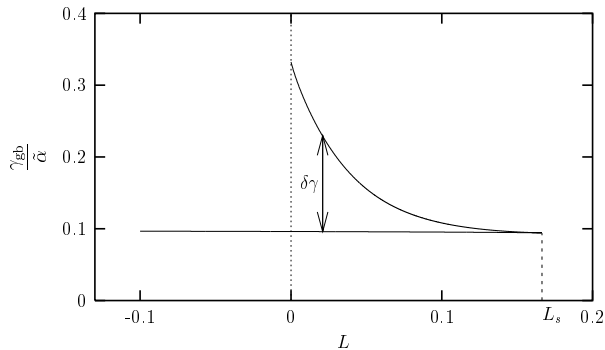


FIG. 3: Energy γ_{gb} in units of $\tilde{\alpha}$ of the low-angle grain boundary (same values of the parameters as in Fig. 2) and the saddle point solution (upper branch).

A. $h = \phi^2$

A typical dependence of the amount of liquid W on temperature L for a low-angle boundary is shown in Fig. 2. The meaning of the “low-angle” will become apparent in a moment. Below the melting temperature $L < 0$, the narrow, dry boundary is the only solution. Above the melting temperature, the narrow, dry boundary is metastable with respect to the uniform fluid. The second solution (upper branch) is the saddle point on the path from the narrow boundary to the globally stable uniform fluid. It gives the size of the critical nucleus. The energy barrier for nucleation $\delta\gamma$ shown in Fig. 3 vanishes at the spinodal temperature L_s above which the grain boundary cannot exist. Note that since the width of the saddle point solution (critical nucleus size) diverges (logarithmically [22]) at the melting temperature, the energy of the saddle point solution must approach that of the two liquid solid interfaces

$$2\gamma_{\text{ls}} = 2\tilde{\alpha} \int_0^1 d\phi \sqrt{2f} = \frac{\tilde{\alpha}}{3}, \quad (10)$$

which it indeed does.

The spinodal temperature’s dependence on \tilde{s} and the misorientation $\Delta\theta$ is shown in Fig. 4. As expected the

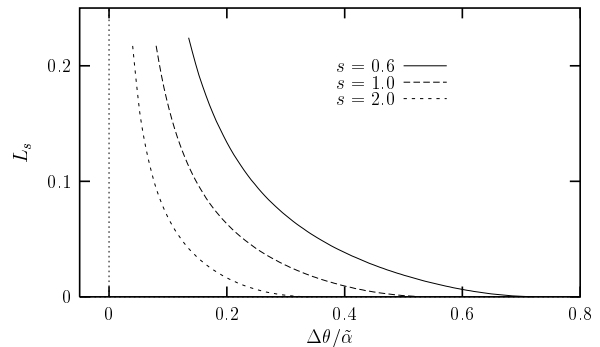


FIG. 4: The spinodal temperature L_s , above which the grain boundary cannot exist, as a function of the misorientation. Note that the spinodal temperature vanishes at a critical misorientation.

spinodal temperature vanishes at an \tilde{s} -dependent critical misorientation $\Delta\theta_c$. Therefore, high-angle grain boundaries ($\Delta\theta > \Delta\theta_c$) cannot exist above the melting temperature. For these boundaries, the amount of fluid W diverges as the melting point is approached from below. Another way to define this critical misorientation is to notice that the energy γ_{gb} of all high-angle grain boundaries approach that of two liquid-solid interfaces (10) at the melting point, whereas low-angle grain boundaries are less energetically costly.

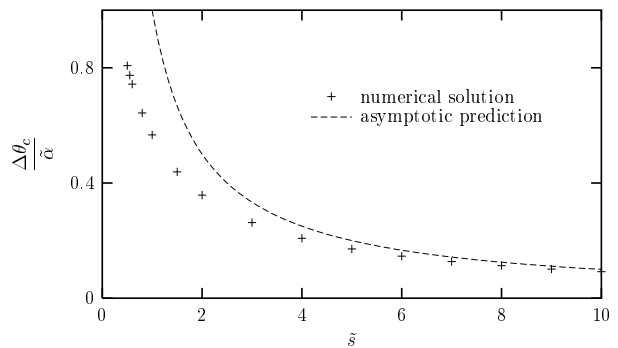


FIG. 5: Critical misorientation in units of α as function of \tilde{s} . $h = \phi^2$. Solid line is the analytic result in the limit of large \tilde{s} .

The dependence of the critical misorientation on \tilde{s} , shown in Fig. 5, can be calculated approximately in the limit of large \tilde{s} . We need to find the largest misorientation for which a solution to (4) exists at the melting point $L = 0$. Using the approximate expression for the right hand side of Eq. (4), calculated in [19], we obtain (ϕ subscript denotes differentiation)

$$\frac{\Delta\theta}{\alpha} \approx \frac{2}{\tilde{s}} \frac{\sqrt{f(\phi_{\text{min}})}}{g_\phi(\phi_{\text{min}})} = \frac{1 - \phi_{\text{min}}}{\tilde{s}}. \quad (11)$$

And since ϕ is restricted to lie within the $[0, 1]$ interval,

a solution only exists for

$$\Delta\theta \leq \Delta\theta_c = \frac{\tilde{\alpha}}{\tilde{s}}. \quad (12)$$

Indeed, for large \tilde{s} the numerically found critical misorientation shown in Fig. 5 approaches this prediction. It is worth noting that no solutions to our model exist for $\tilde{s} < 0.5$. In this case, some values of $\phi_{\min} < 1$ result in unphysical ϕ_{\max} according to Eq. (3).

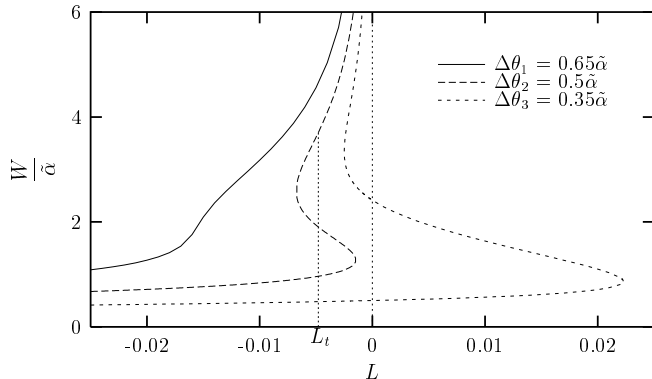


FIG. 6: Amount of liquid W for $h = 1$ in units of $\tilde{\alpha}$ as function of temperature L for $\tilde{s} = 1$ and three different misorientations $\Delta\theta_u < \Delta\theta_1$, $\Delta\theta_l < \Delta\theta_2 < \Delta\theta_u$ and $\Delta\theta_3 < \Delta\theta_l$.

B. $h = 1$

The behavior of W is more complex in this case. As shown in Fig. 6 there are three distinct cases. The amount of liquid at a high-angle boundary diverges smoothly at the melting point. When $\Delta\theta$ is below an upper critical misorientation $\Delta\theta_u$, there is a range of temperatures below melting in which there are two solutions, one stable and one metastable. For example, by looking at the energies of these solutions, we discover, that the narrow, dry solution is stable up to the transition temperature $L_t < 0$ (see Fig. 6). Above this transition temperature, the wide, wet solution is stable, while the narrow, dry solution is metastable. The transition from narrow, dry boundary to wide, wet boundary is discontinuous.

Below a lower critical misorientation $\Delta\theta_l$, there is still a region of temperatures in which there exists a wide, wet solution, but the narrow, dry solution is stable all the way up to the melting temperature.

This definition of the upper and lower critical misorientations lends itself well to predicting the result of raising the temperature slowly. According to our definition, a low-angle grain boundary ($\Delta\theta < \Delta\theta_l$) will remain narrow up the melting point where it will melt via a first order activated transition. Boundaries with intermediate misorientations ($\Delta\theta_l < \Delta\theta < \Delta\theta_u$) will experience a discontinuous jump in width at some characteristic temperature $L_t < 0$. When the temperature is increased

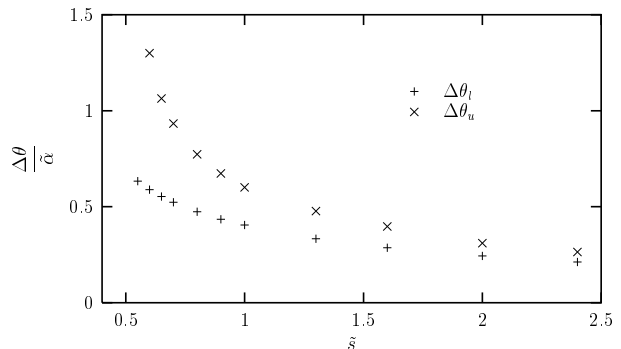


FIG. 7: Upper and lower critical misorientations as a function of \tilde{s} for the $h = 1$ case.

further, the width of the liquid layer will diverge logarithmically at the melting point. High-angle boundaries ($\Delta\theta > \Delta\theta_u$) experience a smooth divergence of the width of the liquid layer as the melting point is approached. The dependence of the lower and upper critical misorientations on \tilde{s} is shown in Fig. 7.

IV. GRAIN BOUNDARY MOBILITY

In this paper we would like to illustrate the flexibility of our model by demonstrating that the choice of model functions is sufficient to reproduce a wide range of behaviors observed experimentally and numerically. For example, molecular dynamics simulations [23] as well as experiments [24] reveal that the mobility of tilt grain boundaries vanishes quickly at the zero misorientation. The same studies find (in two dimensions) a sharp peak in the mobility at special (high coincident site density) misorientations at which the energy of the boundary has a cusp.

As we showed in Ref. [19], within our model, curved boundaries move with a normal velocity proportional to their curvature, energy γ_{gb} and mobility \mathcal{M} which we computed in the sharp interface limit

$$\begin{aligned} \frac{1}{\mathcal{M}} &= \tilde{\alpha}\tilde{s}^2\tilde{\tau}_\theta \int_{\phi_{\min}}^{\phi_{\max}} d\phi P \frac{\phi^2(g(\phi_{\max}) - g)^2}{h^2\sqrt{2f - \tilde{s}^2(g(\phi_{\max}) - g)^2/h}} \\ &+ \frac{\tilde{\tau}_\phi}{\tilde{\alpha}} \int_{\phi_{\min}}^{\phi_{\max}} d\phi Q \sqrt{2f - \tilde{s}^2(g(\phi_{\max}) - g)^2/h} \\ &+ \frac{\tilde{\tau}_\phi}{\tilde{\alpha}} \int_{\phi_{\max}}^1 d\phi Q \sqrt{2f}, \end{aligned} \quad (13)$$

where $\tilde{\tau}_\phi = \tau_\phi/\epsilon^2$ and $\tilde{\tau}_\theta = \tau_\theta/\epsilon^2$.

We studied the scaling of the mobility in the limit of the vanishing misorientation $\Delta\theta$ and found that this limit is governed by the behavior of the model functions near $\phi = 1$. In this paper g and h are regular at $\phi = 1$. Therefore, the behavior of P and Q near $\phi = 1$ determines the scaling of the grain boundary mobility \mathcal{M} for small misorientations. If the most strongly divergent one of the

two functions P and Q behaves like $(1 - \phi)^{-\mu}$, then the mobility scales like $(\Delta\theta)^{2-\mu}$. As we remarked in [19], the divergence of P and Q at $\phi = 1$ is physically plausible since we expect the dynamics of ϕ and θ to slow down in the grain interior.

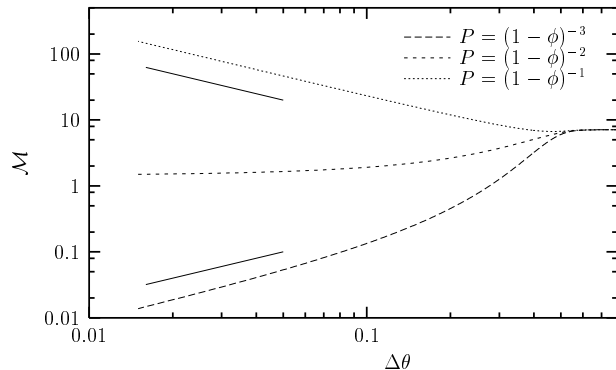


FIG. 8: Grain boundary mobility \mathcal{M} as a function of misorientation both in units of $\tilde{\alpha}$ for $h = \phi^2$ and three choices of P . The slopes of the two straight line segments are $+1$ and -1 . Temperature is $L = -0.001$, $\tilde{s} = \tilde{\alpha} = 1$. Note that above the critical angle, different P makes does not influence the grain boundary mobility.

In Fig. 8 we show the grain boundary mobility as a function of misorientation for $h = \phi^2$, $Q = -\log(1 - \phi)$ and three different choices of P . Indeed, the behavior of P near $\phi = 1$ dictates whether the mobility \mathcal{M} vanishes or diverges at zero misorientation. The undercooling $L = -0.001$ is small in this figure. Larger undercoolings do not alter the qualitative features of the situation. Our model can therefore be adjusted to describe systems in which the mobility dips at small misorientations as well as systems which exhibit peaks in the mobility at special misorientations.

Since the grain boundary mobility is strongly dependent on the amount of disorder W , its behavior as a function of temperature can be inferred from its behavior as a function of misorientation. Specifically, when $\mu > 2$, the mobility is an increasing function of the amount of disorder. And vice versa \mathcal{M} is a decreasing function of W when $\mu < 2$. The amount of disordered material at the grain boundary grows with increasing temperature as well as with increasing misorientation. We therefore expect the mobility to be an increasing function of temperature when $\mu > 2$.

To illustrate this point we set $h = 1$ and plot in Fig. 9 the mobility of a grain boundary which undergoes a discontinuous premelting transition, corresponding to $\Delta\theta_2$ in Fig. 6 ($\Delta\theta_l < \Delta\theta_2 < \Delta\theta_u$). We also choose $\mu = 3$ so that narrow boundaries move slower. The mobility of the narrow, dry boundary, which is stable below L_t , is significantly smaller than that of the wide, wet boundary. Thus when the boundary undergoes the transition it will suddenly accelerate to almost twice the speed.

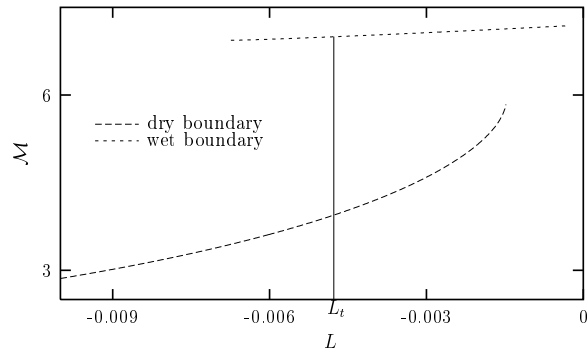


FIG. 9: Mobilities of the wet and dry boundary solutions. Here $\tilde{s} = \tilde{\alpha} = 1$, $\Delta\theta = 0.5\tilde{\alpha}$ and $h = \phi^2$.

V. CONCLUSIONS

In this article we explored the properties of a phase field model of crystal grains. The model is constructed by introducing an order parameter ϕ which measures the degree of disorder (or “fluidity”) and the average local orientation θ . When the phenomenological free energy contains a term which is linear in $|\nabla\theta|$, its relaxational kinetics is singular and has to be interpreted with the help of the extended gradient theory. The relaxing solutions thus obtained are interpreted as a collection of grains in which θ is spatially uniform, separated by narrow grain boundaries.

Our main goal was to demonstrate the ability of this phase field model to reproduce experimentally observed behaviors of grain boundaries. Since our model treats solid grain boundaries and liquid-solid interfaces within a unified framework, it ought to correctly describe the premelting transition of grain boundaries. We indeed find that depending on the choice of the model functions the grain boundary undergoes either a continuous or a discontinuous premelting transition.

If we choose the coefficient of $(\nabla\theta)^2$ in the free energy to be $h(\phi) = \phi^2$, the transition is continuous. This means that there exists a critical misorientation $\Delta\theta_c$ such that grain boundaries with lower misorientations remain narrow and dry all the way up to the melting temperature. When the misorientation is larger than critical, grain boundaries develop a layer of fluid whose width diverges at the melting temperature as the logarithm of the undercooling. The logarithmic divergence is a consequence of the short range interaction of liquid-solid interfaces within this theory.

When $h = 1$, there is a range of misorientations for which the width of the liquid film undergoes a jump at some characteristic temperature below the melting temperature. If the temperature is raised further, the width of the liquid film diverges logarithmically as before. Low angle grain boundaries remain dry and narrow as before. The jump in the width of the fluid layer is due to the details of the short-range interaction of the two liquid solid

interfaces and should be observable in some real systems.

Finally, we have shown that by adjusting the nature of the divergence of the model function P we are able to obtain a wide range of behaviors of the grain boundary mobility. In particular, depending on the exponent of the divergence of P near $\phi = 1$, the mobility of the grain boundary can either vanish at the zero misorientation or it can diverge. Thus the model can emulate the behavior of the mobility observed experimentally near the special

misorientations as well as near the zero misorientation.

In principle, by introducing appropriate additional terms in the free energy, one can construct a more realistic model in which the grain boundary energy has many minima at special misorientations in addition to the cusp at the zero misorientation. It would then be possible to choose P and Q to ensure appropriate peaks or zeroes of the grain boundary mobility at the special misorientations as well as the zero misorientation.

-
- [1] J. C. M. Li, J. Appl. Phys. **33**(10), 2958 (1961).
 [2] J. Q. Broughton and G. H. Gilmer, Model. Simul. Mater. Sci. Eng. **6**, 87 (1998).
 [3] P. Keblinski, D. Wolf, S. R. Phillpot, and H. Gleiter, Philos. Mag. A **79**(11), 2735 (1999).
 [4] T. Nguyen, P. S. Ho, T. Kwok, C. Nitta, and S. Yip, Phys. Rev. B **46**(10), 6050 (1992).
 [5] B. Schonfelder, D. Wolf, S. R. Phillpot, and M. Furtkamp, Interface Sci. **5**(4), 245 (1997).
 [6] T. E. Hsieh and R. W. Balluffi, Acta Metall. **37**(6), 1637 (1989).
 [7] D. M. Zhu and J. G. Dash, Phys. Rev. B **38**(16), 11673 (1988).
 [8] R. A. Masamura, M. E. Glicksman, and C. L. Vold, Scripta Met. **6**, 943 (1972).
 [9] C. L. Vold and M. E. Glicksman, in *The nature and behavior of grain boundaries*, edited by H. Hu, Metallurgical Society of AIME (Plenum Press, New York, 1972), pp. 171–83.
 [10] M. E. Glicksman and C. L. Vold, Acta. Met. **17**, 1 (1969).
 [11] K. T. Author and D. W. Demianczuk, Acta Metall. **23**(10), 1149 (1975).
 [12] T. Watanabe, S.-I. Kimura, and S. Karashima, Philos. Mag. A **49**(6), 845 (1984).
 [13] E. Budke, T. Surholt, S. I. Prokofjev, L. S. Shvindlerman, and C. Herzig, Acta Mater. **47**(2), 385 (1999).
 [14] J. G. Dash, Contemporary Physics **30**(2), 89 (1989).
 [15] D. E. Sullivan and M. M. T. de Gamma, in *Fluid interfacial phenomena*, edited by C. A. Croxton (Wiley, 1986).
 [16] R. Kikuchi and J. W. Cahn, Phys. Rev. B **21**(5), 1893 (1980).
 [17] M. Elbaum and M. Schick, Phys. Rev. Lett. **66**(13), 1713 (1991).
 [18] R. Kobayashi, J. A. Warren, and W. C. Carter, Physica D **140**, 141 (2000).
 [19] A. E. Lobkovsky and J. A. Warren, Phys. Rev. E **63**, 051605 (2001).
 [20] J. S. Langer, in *Directions in condensed matter physics* (World Scientific, Philadelphia, 1986), pp. 164–186.
 [21] W. T. Read and W. Shockley, Phys. Rev. **78**(3), 275 (1950).
 [22] A. E. Lobkovsky and J. A. Warren, in *Influences of Interface and Dislocation Behavior on Microstructure Evolution* (MRS, 2000), vol. 652.
 [23] M. Upmanyu, D. J. Srolovitz, L. S. Shvindlerman, and G. Gottstein, Acta Mat. **47**(14), 3901 (1999).
 [24] G. Gottstein, D. A. Molodov, and L. S. Shvindlerman, Interface Sci. **6**(1-2), 7 (1998).